AD-A120 097 BRUNEL UNIV UXBRIDGE (ENGLAND) DEPT OF NON-METALLIC --ETC F/G 11/9
CRYSTALLINE DEFECTS AND DEFORMATION MECHANISMS IN SEMI-CRYSTALL--ETC(U)
MAY 82 A HUNTER, M BEVIS DAJA37-80-C-0497

UNCLASSIFIED NL

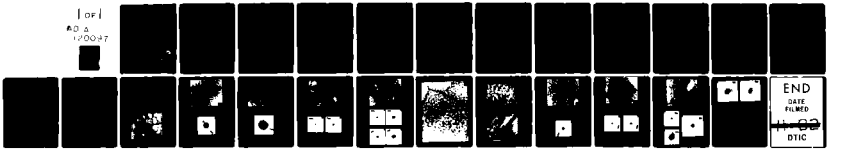

AD

CRYSTALLINE DEFECTS AND DEFORMATION MECHANISMS IN SEMI-CRYSTALLINE POLYMERS

Final Technical Report

by

A. Hunter and M. Bevis

May, 1982

United States Army

Research & Standardization Group (Europe)

London : England

Contract Number: DAJA 37-80-C-0497

BRUNEL UNIVERSITY

AD

CRYSTALLINE DEFECTS AND DEFORMATION MECHANISMS IN SEMI-CRYSTALLINE POLYMERS

Final Technical Report

by

A. Hunter and M. Bevis

May, 1982

United States Army

Research & Standardization Group (Europe)

London : England

Contract Number: DAJA 37-80-C-0497

BRUNEL UNIVERSITY

UNCLASSIFIED

SECURITY CLASSIFICATION OF THIS PAGE (When Data Entered)

R & D 2625-MS

REPORT DOCUMENTATION PAGE		READ INSTRUCTIONS BEFORE COMPLETING FORM
1. REPORT NUMBER	2. GOVT ACCESSION NO. AD A120 097	3. RECIPIENT'S CATALOG NUMBER
4. TITLE (and Subtitle) Crystalline Defects and Deformation Mechanisms in Semi-Crystalline Polymers		5. TYPE OF REPORT & PERIOD COVERED Final Technical Report 1 Sept 80 - 31 May 82
		6. PERFORMING ORG. REPORT NUMBER
7. AUTHOR(s) A. Hunter and M. Bevis		8. CONTRACT OR GRANT NUMBER(s) DAJA37-80-C-0497
9. PERFORMING ORGANIZATION NAME AND ADDRESS Department of Non-Metallic Materials Brunel University Uxbridge, Middlesex		10. PROGRAM ELEMENT, PROJECT, TASK AREA & WORK UNIT NUMBERS IT161102BH57-04
11. CONTROLLING OFFICE NAME AND ADDRESS USARDSG-UK Box 65 FPO New York 09510		12. REPORT DATE May 1982
		13. NUMBER OF PAGES 20
14. MONITORING AGENCY NAME & ADDRESS(if different from Controlling Office)		15. SECURITY CLASS. (of this report) UNCLASSIFIED
		15a. DECLASSIFICATION/DOWNGRADING SCHEDULE

16. DISTRIBUTION STATEMENT (of this Report)

Approved for public release; Distribution unlimited

17. DISTRIBUTION STATEMENT (of the abstract entered in Block 20, if different from Report)

18. SUPPLEMENTARY NOTES

19. KEY WORDS (Continue on reverse side if necessary and identify by block number)

Polyethylene, spherulites, deformation, scanning transmission, electron microscopy, twinning, martensitic transformations.

20. ABSTRACT (Continue on reverse side if necessary and identify by block number)

The microstructure and subsequent mechanisms of deformation in polyethylene spherulites is very dependent on the method of spherulitic film preparation. Slowly cooled spherulites have been previously investigated in detail by transmission electron microscopy and diffraction, whereas the present work has been primarily concerned with the reproducible preparation of rapidly cooled high density polyethylene films which exhibit a banded spherulite morphology. Techniques for the preparation of deformed thin polyethylene

DD FORM 1 JAN 73 1473 EDITION OF 1 NOV 65 IS OBSOLETE
S/N 0102-LF-014-6601

UNCLASSIFIED
SECURITY CLASSIFICATION OF THIS PAGE (When Data Entered)

20. Cont...films and their subsequent examination by scanning transmission electron microscopy and diffraction have been developed. Fine differences in the spherulite morphology have been identified, as ' .e the differences between the operative deformation mechanisms in rapidly and slowly cooled spherulitic films.

CRYSTALLINE DEFECTS AND DEFORMATION MECHANISMS IN SEMI-CRYSTALLINE POLYMERS

Principal Investigator: Professor M.Bevis

Research Contract: DAJA 37-80-C-0497.

Final Report

1 September 1980 - 31 May 1982

The Research reported in this document has been made possible through the support and sponsorship of the U.S. Government through its U.S. Army Research and Standardisation Group (Europe).

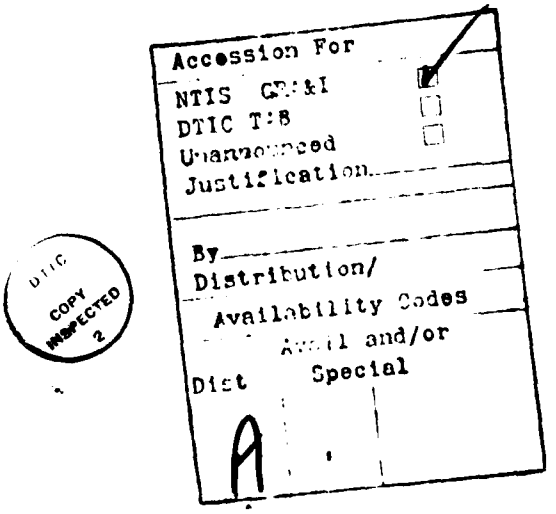

ABSTRACT.

The microstructure and subsequent mechanisms of deformation in polyethylene spherulites is very dependent on the method of spherulitic film preparation. Slowly cooled spherulites have been previously investigated in detail by transmission electron microscopy and diffraction, whereas the present work has been primarily concerned with the reproducible preparation of rapidly cooled high density polyethylene films which exhibit a banded spherulite morphology. Techniques for the preparation of deformed thin polyethylene films and their subsequent examination by scanning transmission electron microscopy and diffraction have been developed. Fine differences in the spherulite morphology have been identified, as have the differences between the operative deformation mechanisms in rapidly and slowly cooled spherulitic films.

Keywords: Polyethylene, spherulites, deformation, scanning transmission electron microscopy, twinning, martensitic transformations.

Table of Contents.

1. Introduction

The main objectives of the early stages of the research was to establish experimental bases for the preparation of thin high density polyethylene (HDPE) films suitable for transmission electron microscopy, the deformation of such thin films and the subsequent recording of electron diffraction patterns and electron images. The reported success in specimen preparation was short lived.

Crystallisation conditions are known to have a marked effect on the microstructure and mechanical properties of polyethylene spherulites (1). Previous studies have investigated the deformation mechanisms operative in slowly cooled (S) thin films (2,3) whereas in the present programme the objective was to investigate the deformation of rapidly cooled (R) polyethylene spherulites which have a characteristic banded morphology. Considerable experimental work was required to reproducibly gain polyethylene spherulitic films with banded morphology. The procedures which are summarised below enabled thin films to be made and subsequently deformed in reproducible ways.

2. Experimetal

Preparation of R type high density polyethylene thin films possessing a 'banded' spherulite morphology.

The most satisfactory method of preparing R type PE thin films suitable for deformation studies was found to be solvent casting a dilute, boiling solution of the polymer directly onto an extensible substrate.

In order to control the crystallisation parameters, a special hot-plate was constructed, according to the schematic diagram in figure 1. The temperature of the hot-plate and substrate film could be carefully controlled by pre-heating in an oven.

The hot-plate was constructed of mild steel and had a large thermal capacity. It was fashioned as an 'open-ended box' into which a thin Mylar strip could be inserted. A 2.5mm diameter hole drilled in the centre of the top plate would allow a micro-pipette access to the Mylar strip. Thus, the solvent casing could be carefully controlled, and, for example, draughts were excluded. A 1mm slow was cut along the length of the top plate, passing through the 2.5mm hole. This allowed a visual inspection of the liquid deposition.

The internal surfaces of the hot-plate were ground flat on a surface grinder to ensure good thermal contact between the Mylar strip and the bottom plate and also good thermal transfer to the Mylar strip.

Prior to solvent casting, the Mylar strip and hot plate were pre-heated to a relatively high temperature (about 160°C). After removal from the oven two or three drops of a boiling 0.4% solution w/w of HDPE in Xylene were deposited onto the Mylar strip through the 2.5mm hole. After 2 mins the strip was removed from the hot plate and allowed to cool to room temperature.

The resulting R-type polyethylene thin films were always of a very even thickness and showed a spherulitic-banded structure upon examination by transmitted light microscopy using cross polars. The photograph in figure 2 shows a banded structure typical of that gained using the technique described above, and subsequently used for deformation studies.

A parallel-sided strip was cut from the Mylar film (~ 0.5 cm wide) and was deformed using a small, hand-operated tensile testing device. The strained specimen was then shadowed with carbon in a direction parallel to the tensile axis. This allows the straining axis to be identified from the transmission electron micrographs. A few drops of Poly Acrylic Acid were deposited onto the PE/carbon film. When the sandwich of PE/C/PAA had hardened it could be removed from the Mylar, and caused the strain on the HDPE to be maintained after stripping from the Mylar. This ensured that the stress-induced twinning, martensitic transformations and slip would be identified by analysis of electron diffraction patterns. The PE face of the sandwich was then lightly scored with a scalpel into squares (~ 2mm square). The sandwich was then allowed to float in distilled water (PE side up) and when the PAA had dissolved the PE/C film could be picked up on copper grids suitable for electron microscopy studies.

A JEOL 120CX transmission electron microscope with STEM attachment was used to investigate the microstructure of deformed and undeformed PE films, as described in the previous progress report. A micro-electron

diffraction technique was used in order to reduce beam damage effects. The use of a small Condenser lens aperture (20μm) enabled electron diffraction patterns from areas as small as $(0.25\ \mu m)^2$. By manipulation of the objective lens current it was possible to contract the stationary beam to the size of the diffracting spot. Thus no selected area aperture was needed, and furthermore during the exposure of a diffraction pattern the beam damage was restricted to the diffracting area under examination. It was therefore possible to obtain many diffraction patterns from a single spherulite. The relatively short "life-time" of the diffraction patterns required the use of X-ray film for the purpose of making recordings.

Diffracting areas could be readily identified by the contamination marks on the surface of the specimen and subsequently recorded in bright field images for analysis.

3. Results

3.1 Spherulite Characterisation

A detailed examination has been made of the 'R type' spherulitic film before and after straining. Figure 3 shows a typical bright-field electron micrograph and contamination marks associated with three electron diffraction patterns, which were taken from three differently oriented radii. The selected area electron diffraction pattern shown was recorded from the indicated contamination mark. The (020) reflection in this case is parallel to the spherulite radius containing the selected area. Similar patterns were recorded from the other two areas in this example, but the patterns were rotated, as in all other films examined, so that the 020 reflections in each case were parallel to the spherulite radius. The arrow shown in all diffraction patterns is parallel to the spherulite radius containing the selected area from which the pattern was obtained.

A greater number of reflections are shown in the electron diffraction pattern shown in figure 4 which was gained from a thinner polyethylene film. The pattern may be indexed by reference to (2). It will be evident from a comparison with the electron diffraction pattern shown in figure 4 and those gained from slowly cooled spherulites and shown in (2), that the crystallographic reflections in 'R' type spherulites are much more diffuse than those in the 'S' type spherulites.

Reference to the contamination marks in figures 3 and 4 will indicate that the selected areas in all cases span both dark and bright bands, and do not, therefore, allow particular features of the bands exhibiting different contrast to be identified. Subsequent experiments using micro-electron diffraction, at the smallest spot size compatible with gaining useful crystallographic information because of beam damage effects, did provide some useful information. Figure 5 shows selected area electron diffraction patterns taken successively along a spherulite radius in a very thin film, in which the bands are barely visible. Substantial differences in the diffraction patterns, in this and other examples not shown here, may be recognised. For example, in one of the patterns the 010 and 110 reflections are much narrower (b) than those shown in the other pattern (a), indicating a more ordered arrangement of crystalline lamellae in the spherulite region (b). This affect is illustrated more clearly in figure 6. The pattern (d) generated from the dark band exhibits broader 110 reflections. Examination of the bright field micrographs (figures 7a and 7b) indicates that the diffracting regions within the bright bands, approximating to dark lines parallel to the spherulite radii and associated with 110 reflections, are more parallel to each other than the much higher concentration occurring in the dark bands. These observations are consistent with those darkfield studies reported previously (4), and are indicative of a marked difference in crystalline lamellae within adjacent bright and dark bands in the 'R' type spherulites.

As a comparison with figures 7(a) and figure 7(b), figure 7(c) shows the morphology of a typical slowly-cooled thin film of HDPE. The 'S' type films were made as described in previous studies (1, 2, 3 & 4).

3.2 Spherulite Deformation Studies.

Preliminary tests were carried out for a range of deformations to gauge the extent of differences between the deformation morphologies of the slowly cooled 'S' (2, 3) and the rapidly cooled 'R' type spherulites. The study showed that there was a marked difference between the response of the two types of spherulitic film to the same deformation. For a given deformation, the stress induced twinning and martensitic transformations (orthorhombic to monoclinic phase) are much less prominent in the 'R' than the 'S' type spherulites. In order to identify the predominant mechanisms of intra-lamellae deformation, 30% strain was selected for detailed investigation.

The main difficulty of working at such relatively high deformations was that after deformation the banded morphology in the 'R' type spherulites was not readily identifiable. The technique adopted to identify differences in deformation behaviour was to take selected area electron diffraction patterns along particular radii. This was done in the equatorial (Region I), polar (Region III) and intermediate regions (Region II) of selected spherulites, which exhibited marked differences in deformation in 'S' type spherulites (2, 3).

A small selection of the results follows:

Region I: Large selected area electron diffraction patterns were obtained from Region I; an example is shown in figures 8(a) and 8(b). From an examination of the diffraction pattern, it is evident that 110 orthorhombic twinning has occurred followed by a 1_1 martensitic transformation of the twinned crystal. Figure 8(b) has been partly indexed to show this.

Region II: Large selected area electron diffraction patterns were obtained from Region II; an example is shown in figure 9(b). As with the 'S' type results (1, 2 & 3) 310 orthorhombic twinning appears to have occurred as well as rotations of the indicated reflections.

Region III: Large selected area electron diffraction patterns were obtained from Region III; an example is shown in figure 9(a). A larger separation of the 110 reflections seems to occur in the 'R' type films (up to 5^{o} more at this deformation).

An attempt has been made to obtain micro-diffraction patterns from the deformed 'R' type film.

Figure 10f shows a portion of a deformed spherulite that has had five micro-diffraction patterns taken from it (clearly labelled).

The group of patterns (10a, b & c) come from Region II and the group of patterns (19d & e) come from Region III. Clearly, there are marked differences in the deformation behaviour along a spherulite radius. An attempt has been made to index the patterns.

4. Conclusions.

The research work described in this report was far more difficult to complete than originally envisaged, and it is clear that a complete picture of the microstructure and mechanisms of deformation in 'R' type spherulites will require considerably more effort. It is likely that the total effort will

match that involved in gaining the references quoted in this report. However, the new work has resulted in some important guidelines. A reproducible experimental technique for making 'R' type spherulitic films has been developed, as have improvements in methods for gaining useful electron micrographs and diffraction patterns from the beam sensitive H.D.P.E. films. These experimental techniques should find application for the investigation of other electron beam sensitive materials.

Together, these have indicated differences in spherulite morphology and deformation mechanisms which should, in future, with more work, allow detailed models to be developed without too much difficulty.

The operation of deformation mechanisms alternative to stress-induced twinning and martensitic transformations play a more important role in the 'R' than the 'S' type spherulites, and this naturally relates to the differences in spherulite morphology - the former being less crystalline overall than the latter. At 40% deformation an 'R' type spherulite exhibits deformation twinning and martensitic transformations in terms of orientation relationships, sequencing and intensity, which would occur at only 25% deformation in 'S' type spherulites.

The fact that the orientation relationships between the undeformed parts of the lamellae within spherulites, the twinned and the martensitically transformed regions, and the sequencing of the multiple deformation mechanisms are similar, indicates that the underlying lamellae structure is similar, in both types of spherulite, at least in part. The electron diffraction patterns do, however, suggest that the complex sequence of deformation mechanisms found in the 'S' type spherulites (2, 3) also occurs in the bright bands of the 'R' type spherulites, and less likely in the dark bands. This tends to support previous observations on the microstructure of the 'R' type spherulites (4).

5. References:

1. Low, A., Vesely, D., Allan, P. and Bevis, M., 1978, J. Mater.Sci. 13, 711.
2. Allan, P. and Bevis, M., 1977, Phil. Mag. 35, 405.
3. Allan, P. and Bevis, M., 1980, Phil. Mag. 41, 555.
4. Low, A., Allan, P., Vesely, D. and Bevis, M., 1977. Inst.Phys.Conf. Ser. No. 36. Chapter 10, 395.

6. Figure Captions.

Fig. 1. Line drawing of the special hot plate that was constructed in order to solvent-cast 'R' type, P.E., thin films directly onto an extensible substrate.

Fig. 2. A bright field scanning transmissiong electron microtraph of an underformed, 'R' type thin film of HDPE. The spherulites exhibit a marked, banded morphology.

Fig. 3(a) A bright field scanning transmission electron micrograph of an underformed, 'R' type thin film showing three contamination marks within a single spherulite.

(b) The selected area electron diffraction pattern recorded from the area indicated by the arrow in figure 3(a). Note that the 020 reflections are parallel to the spherulite radius as indicated by the single-headed arrow in fig. 3(b).

Fig. 4(a) A bright field scanning transmission electron micrograph of a relatively thin underformed, 'R' type film showing a contamination mark.

(b) The selected area electron diffraction pattern recorded from the area indicated in Fig. 4(b).

Fig. 5(a) Micro-diffraction pattern taken from a predominantly dark band of the spherulite shown in Fig. 5(c).

(b) Micro-diffraction pattern taken from a predominantly light band of the spherulite shown in Fig. 5(c).

(c) A bright field scanning transmission electron micrograph of an underformed, relatively thin 'R' type film. Note that the contamination marks (a) and (b) lie approximately along the spherulite radius.

Fig. 6(a) Micro-diffraction pattern taken from a predominantly light band of the spherulite shown in Fig. 5(e)

(b) Ditto

(c) Ditto

(d) Micro-diffraction pattern taken from a predominantly dark band of the spherulite shown in Fig. 5(e).

Figure Captions (Continued).

(e) A bright field scanning transmission electron micrograph of an underformed 'R' type film. The areas where the micro-diffraction patterns 5(a), 5(b), 5(c) and 5(d) were taken from are clearly labelled.

Fig. 7(a) A bright field scanning transmission electron micrograph of an underformed 'R' type film showing the more coherent morphology of dark lines in the light bands. Two large selected-area electron diffraction patterns were taken from this sample.

(b) A bright field scanning transmission electron micrograph of an underformed 'R' type film. Two micro-diffraction patterns were taken from this sample.

(c) A bright field scanning transmission electron micrograph of an 'S' type film.

Fig. 8(a) Bright field scanning transmission electron micrograph of a deformed 'R' type film. The indicated selected area electron diffraction pattern lies in Region I.

(b) Selected area electron diffraction pattern, typical of Region I behaviour at this level of deformation. The double-headed arrow indicates the tensile axis.

Fig. 9(a) Selected area electron diffraction pattern from the indicated area in Fig. 9(c). This pattern is taken from Region III.

(b) Selected area electron diffraction pattern from the area indicated in Fig. 9(c). This pattern is taken from Region II.

(c) Bright field scanning transmission electron micrograph of a deformed 'R' type film. The two large selected area electron diffraction taken from this sample are indicated by their contamination marks.

Fig.10(a) Micro-diffraction pattern (Region II). Thought to come from a predominantly dark band.

(b) Ditto: Thought to come from a predominantly light band.

(c) Ditto: ..... Ditto ..... dark band.

(d) Micro-diffraction pattern (Region III). Thought to come from a predominantly light band.

(e) Ditto: ..... Ditto ..... dark band.

(f) Bright field scanning transmission electron micrograph of a deformed 'R' type film. The contamination marks corresponding to the micro-diffraction patterns 10a - c are labelled.

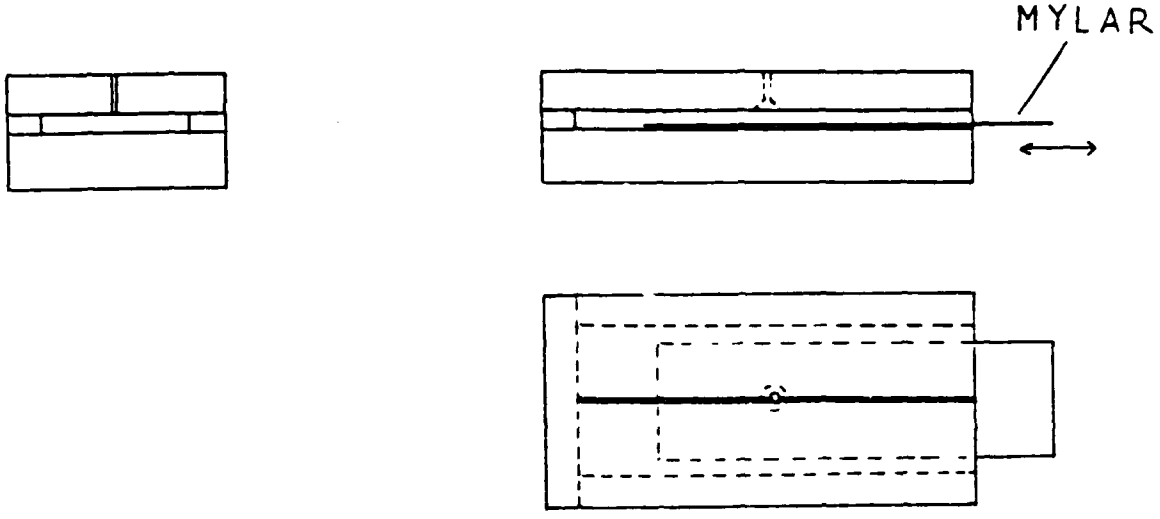

SCALE : 1/2

FIG. 1.

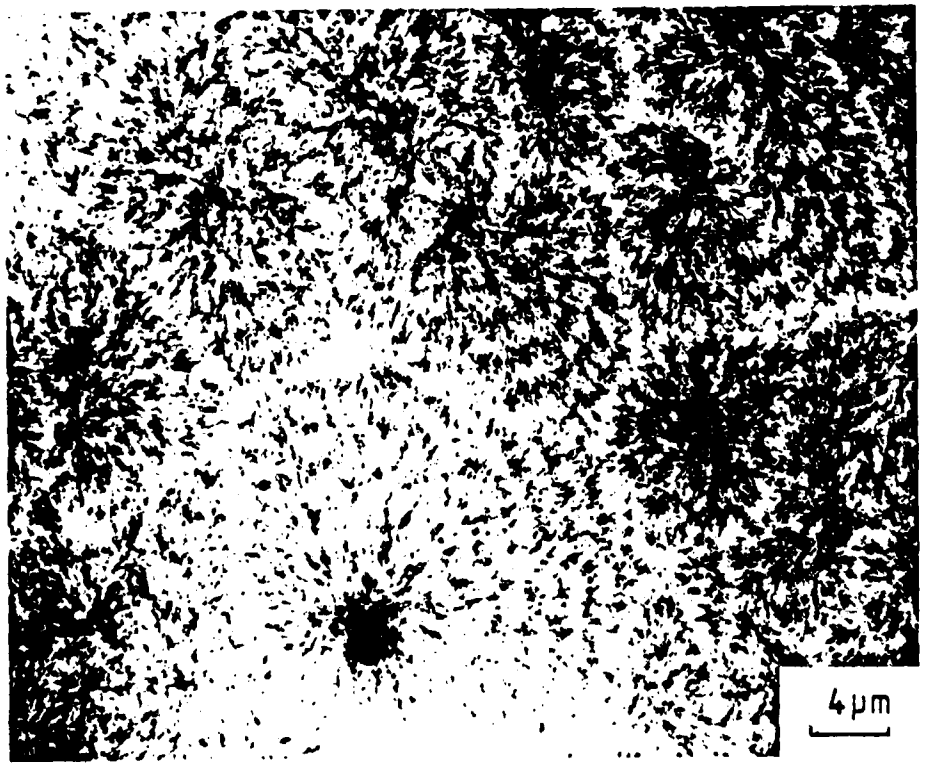

FIG. 2.

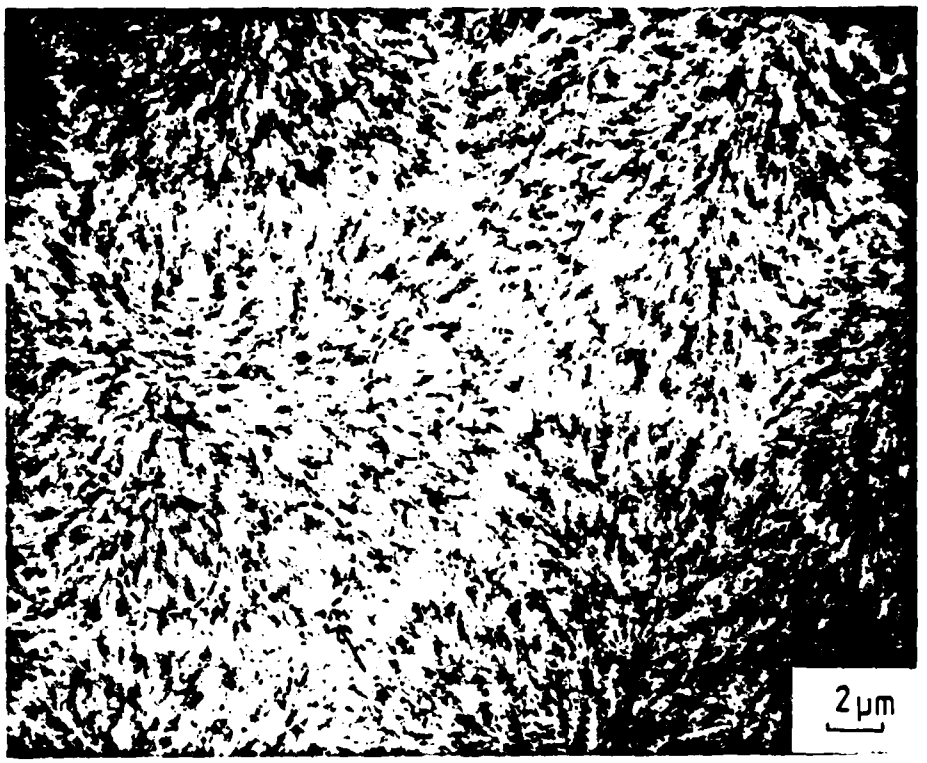

a

b

FIG. 3.

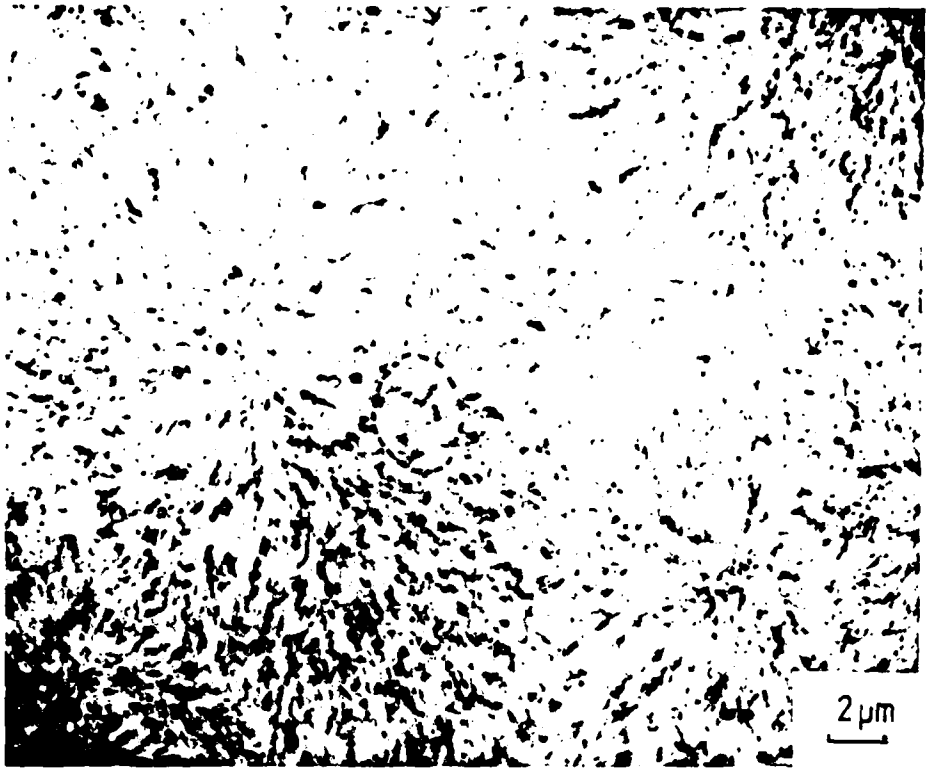

a

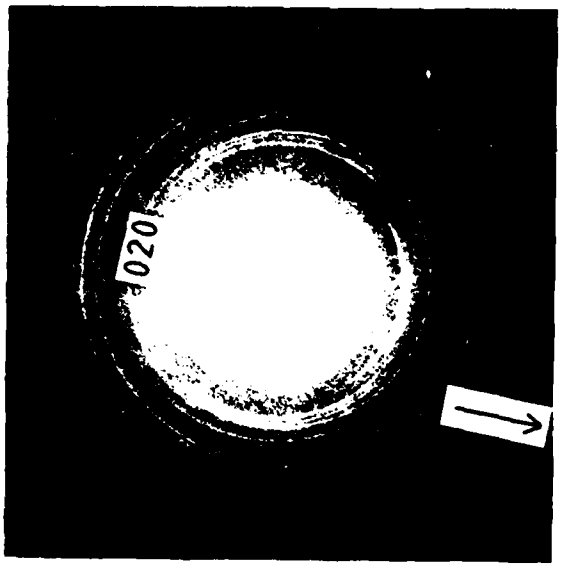

b

FIG. 4.

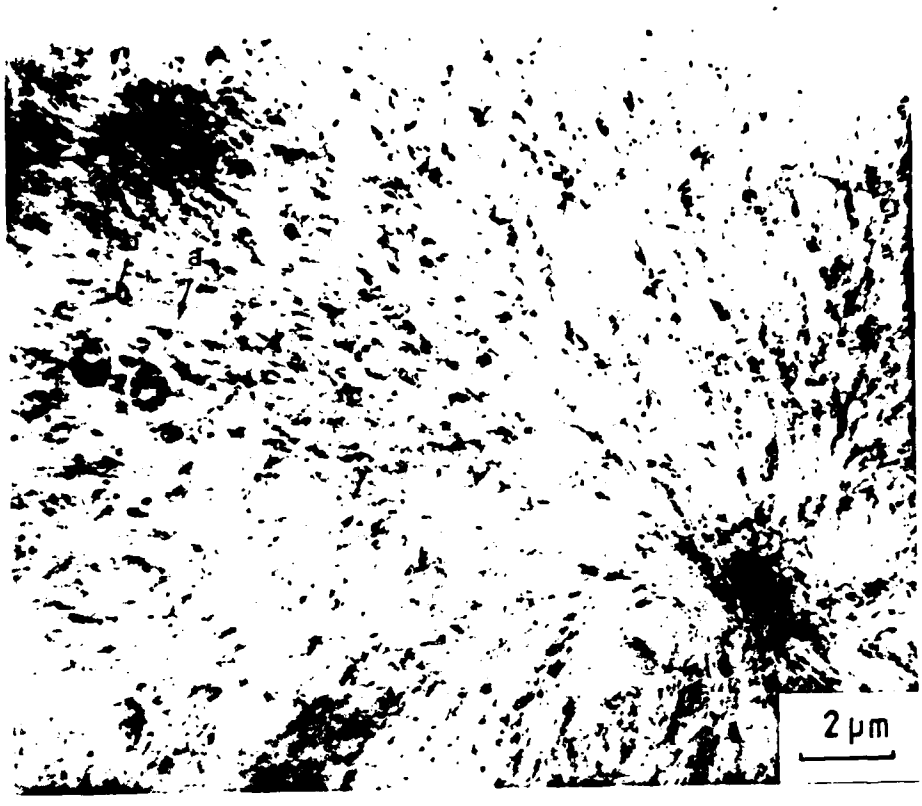

c

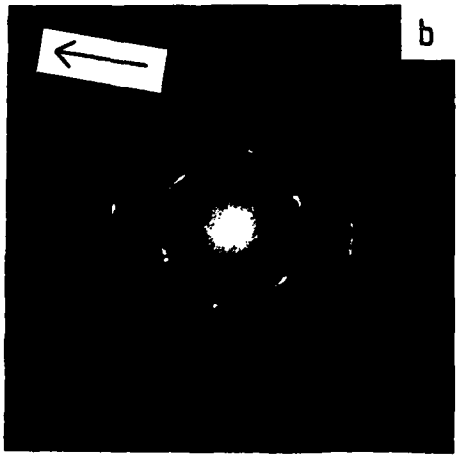

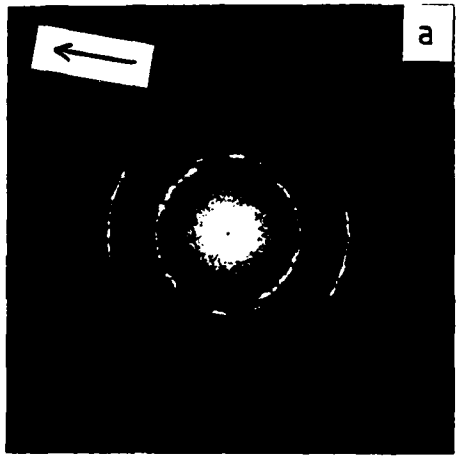

b, a

FIG. 5.

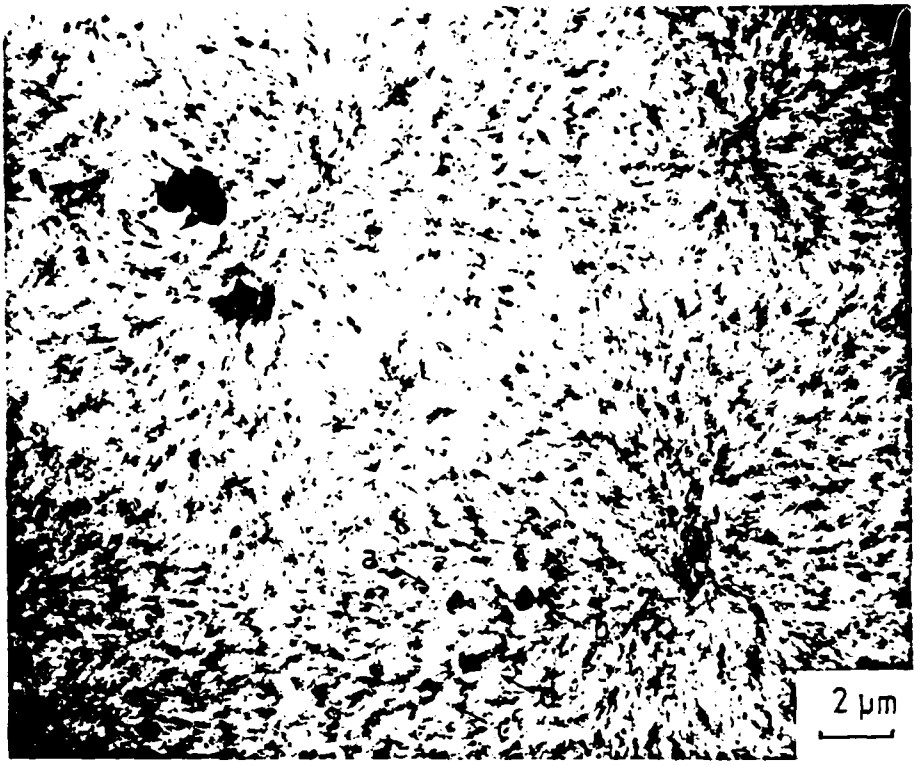

e

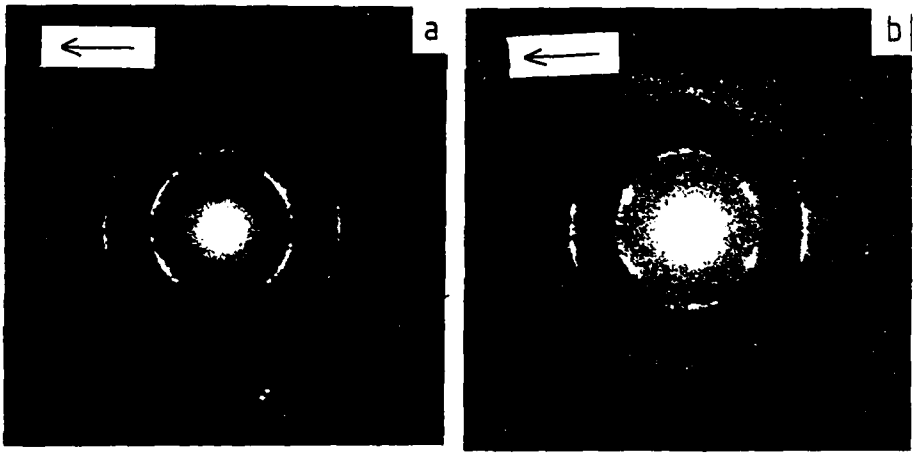

a, b

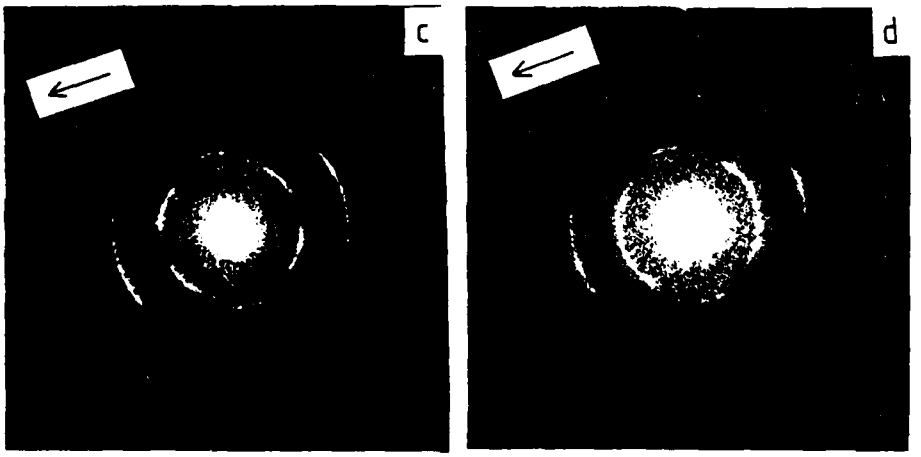

c, d

FIG. 6.

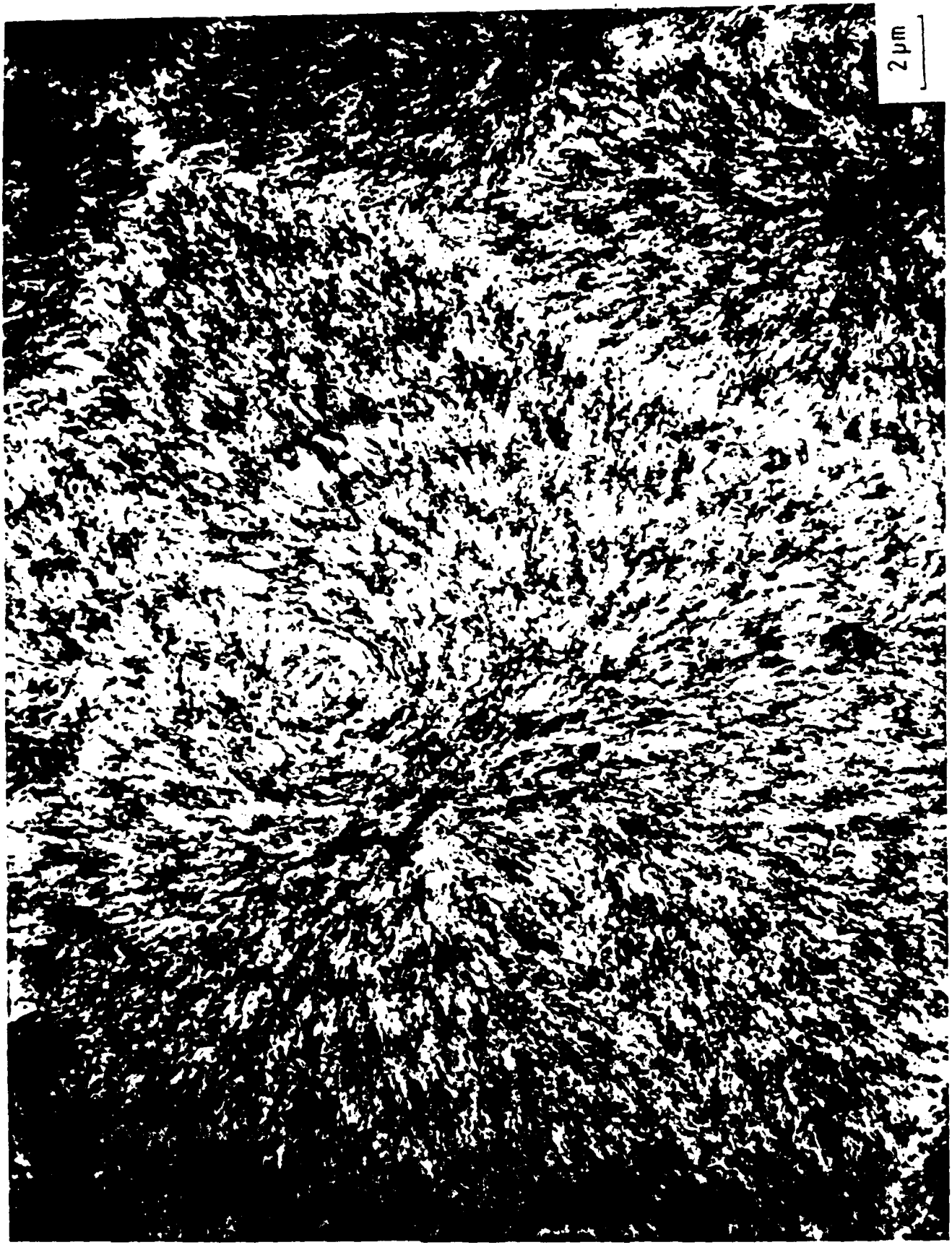

FIG. 7(a)

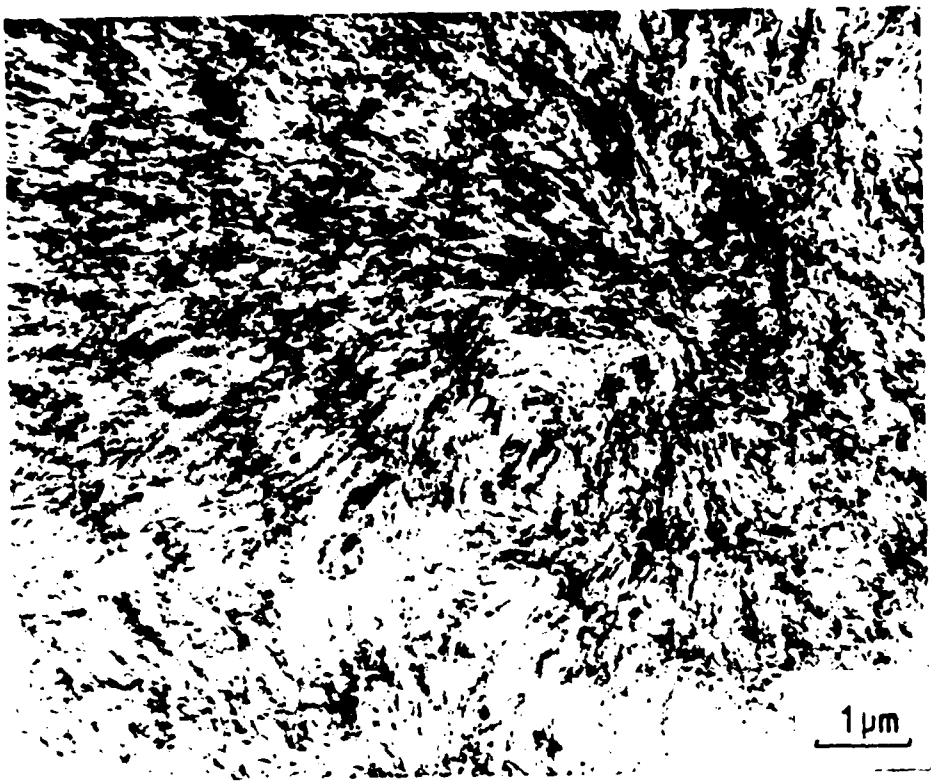

b

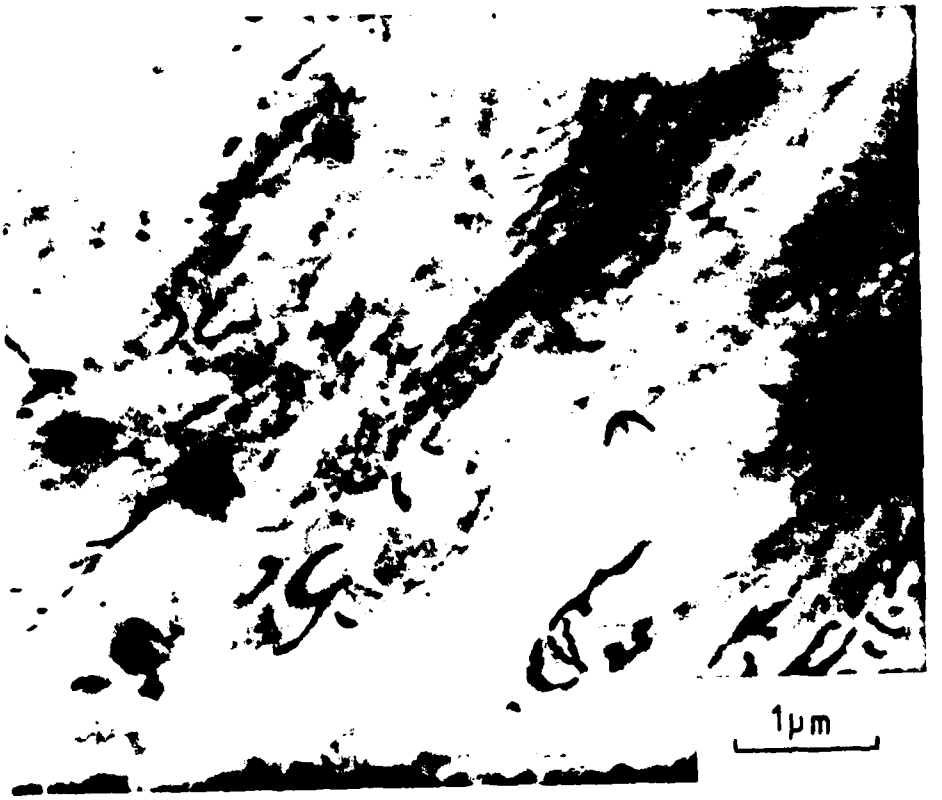

c

FIG.7

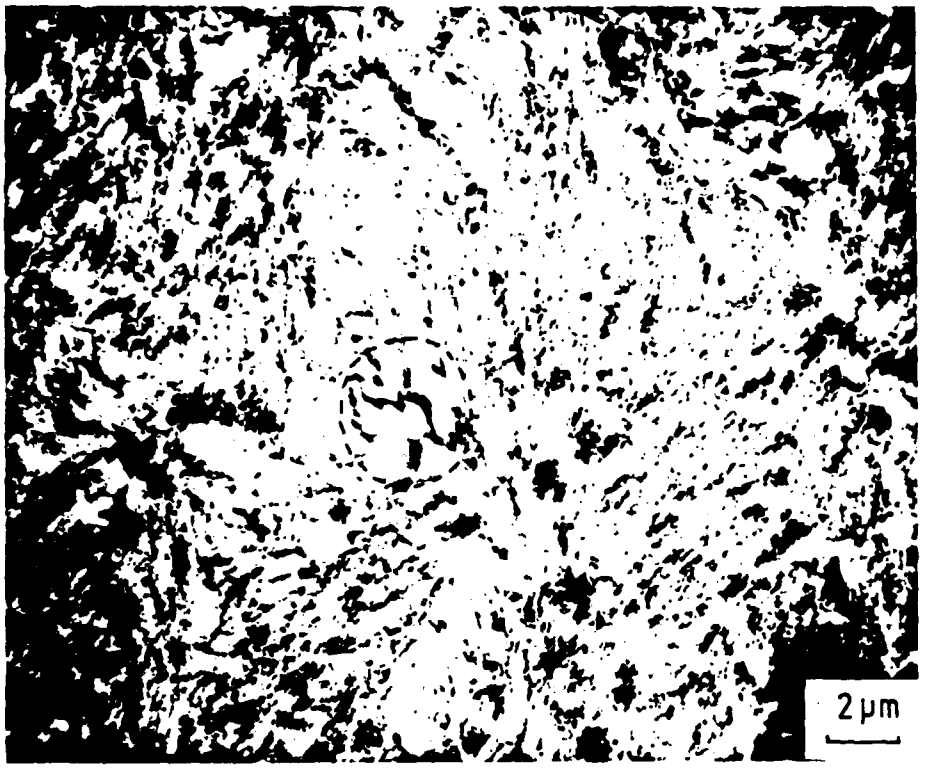

a

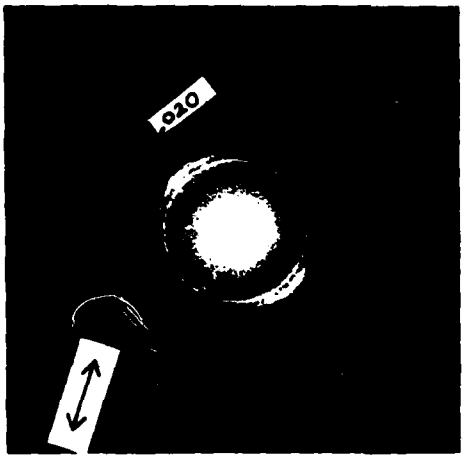

b

FIG.8.

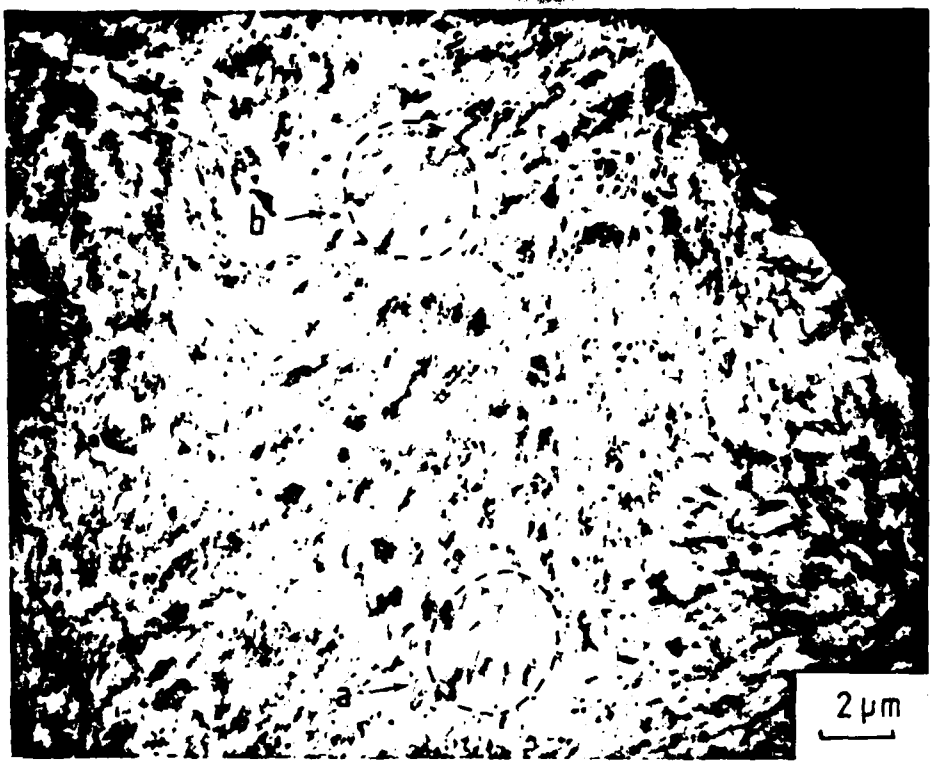

c

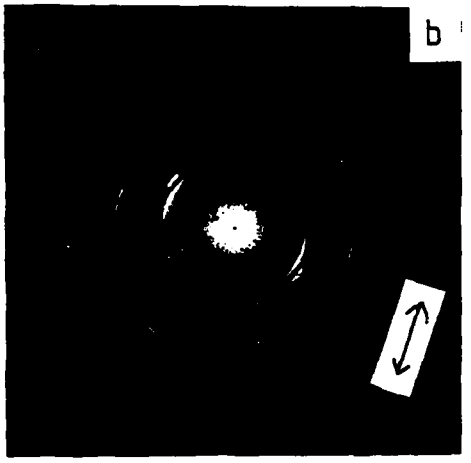

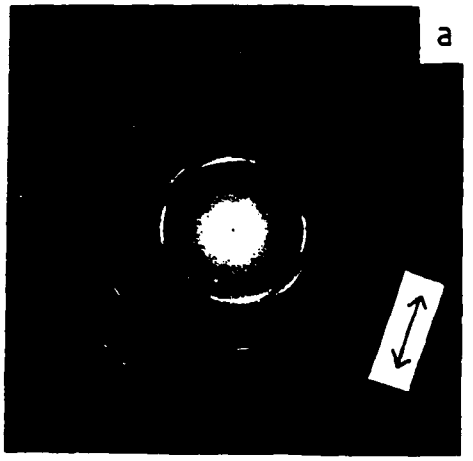

b, a

FIG. 9.

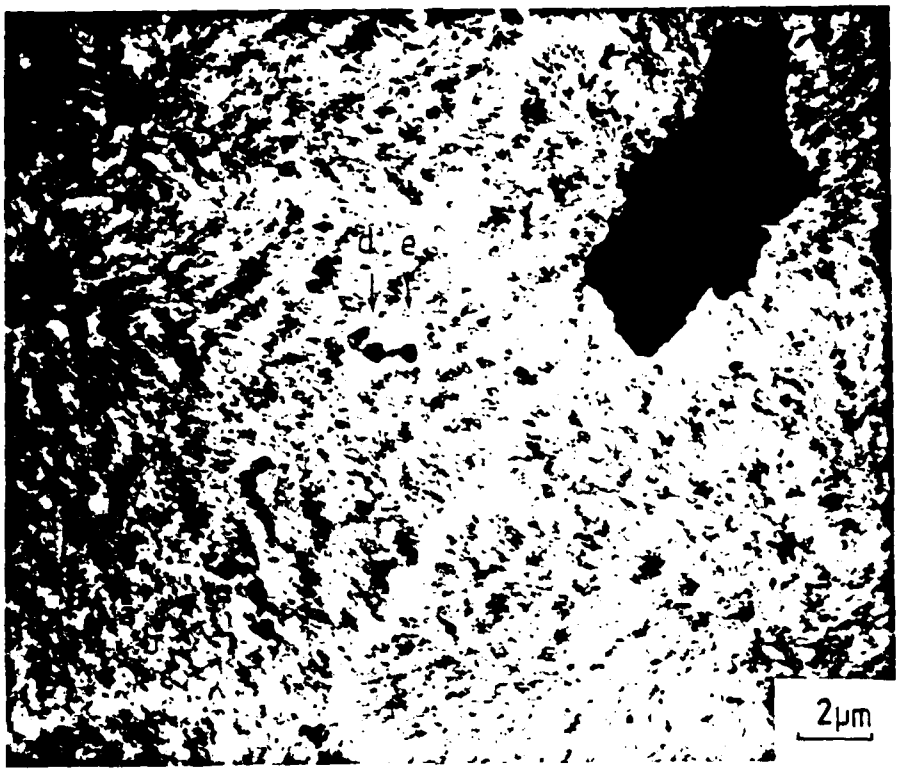

f

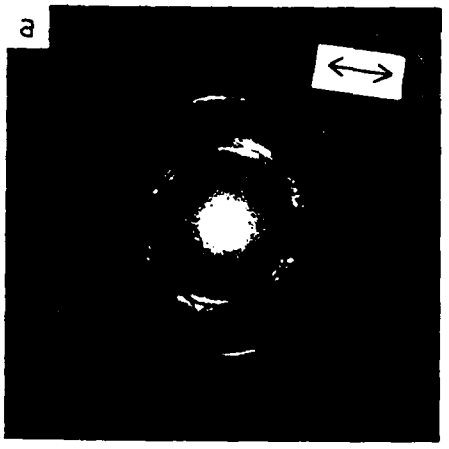

a

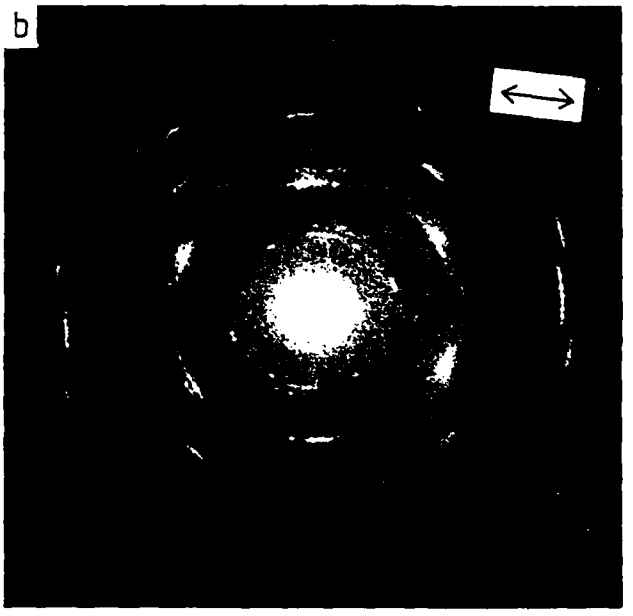

b

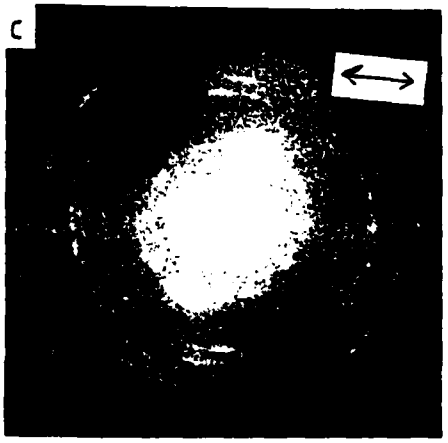

c

FIG.10

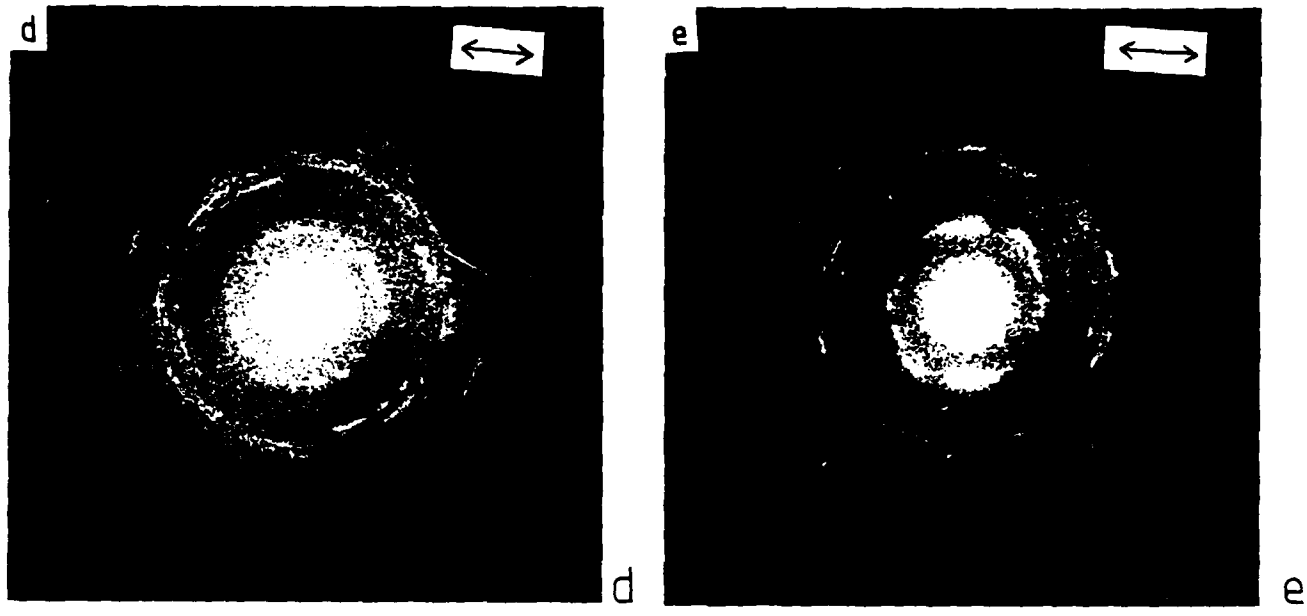

FIG. 10.

END

DATE
FILMED

DTIC